Article

Not peer-reviewed version

Kilovoltage Energy Significantly Enhances the Therapeutic Efficacy of Low-Dose Radiation Against Alzheimer's Disease in 3xTg-AD Mice

Seungwon Lee [†], Ye Jin Yoo [†], Gyehyeong Kim, Eunsu Kim, Subin Yun, Joon Kim, Hoon Ryu [*], Weonkuu Chung [*]

Posted Date: 1 April 2026

doi: 10.20944/preprints202604.0063.v1

Keywords: Alzheimer's disease; low-dose radiation; kilovoltage energy; amyloid-β; tau

 doi:10.20944/preprints202604.0063.v1

Article

Kilovoltage Energy Significantly Enhances the Therapeutic Efficacy of Low-Dose Radiation Against Alzheimer's Disease in 3xTg-AD Mice

Seungwon Lee [1,†], Ye Jin Yoo [1,†], Gyehyeong Kim [1], Eunsu Kim [1], Subin Yun [1], Joon Kim [1], Hoon Ryu [2,*] and Weonkuu Chung [1,*]

[1] Department of Radiation Oncology, Kyung Hee University College of Medicine, Kyung Hee University Hospital at Gangdong, 82 Dongnam-ro Gangdong-gu, Seoul 05278, Republic of Korea

[2] Center for Brain Disorders, Brain Science Institute, Korea Institute of Science and Technology (KIST), 5, Hwarang-ro 14-gil Seongbuk-gu Seoul, 02792 Republic of Korea

* Correspondence: hoonryu@kist.re.kr (H.R.); wkchung@khnmc.or.kr (W.C.)

† These authors contributed equally to this work.

Abstract

Low-dose radiation (LDR) has emerged as a promising therapeutic modality for Alzheimer's Disease (AD). Although different irradiation protocols have been explored, the optimal parameters for maximizing therapeutic efficacy remain unclear. Radiation energy has been shown to influence radiobiological responses, with more pronounced effects at lower energy ranges. We therefore investigated whether kilovoltage LDR (KLDR) provides superior therapeutic efficacy compared with megavoltage LDR (MLDR) in an AD mouse model (3xTg-AD). To this end, we directly compared the efficacy of MLDR and KLDR in AD mice to identify an optimal irradiation strategy for LDR treatment with potential relevance to clinical translation in AD. X-rays with 110-kV or 6-MV energy were applied to the brain of early-stage AD mice (3xTg-AD, 26-28 weeks age) (0.6 Gy × 5 fractions for 2.5 weeks). After LDR treatment, cognitive function was assessed in AD mice using passive avoidance (PA) test and novel object recognition (NOR) test. In addition, different molecular markers associated with inflammation, amyloid-beta (Aβ) plaques, tau burden, and neuronal and synaptic degeneration, were analyzed in the brain of AD mice. KLDR (110 kV) significantly inhibited cognitive decline in AD mice, as demonstrated by both the PA and NOR tests. In addition, KLDR significantly reduced hippocampal levels of GFAP, Iba-1, and pro-inflammatory cytokines (TNF-α and IL-1β), along with marked decreases in Aβ and tau levels. Furthermore, the expression levels of Aβ40 and Aβ42 were quantified by ELISA following KLDR and MLDR treatment, revealing a statistically significant reduction in the KLDR group. The degeneration of neurons and synapses was significantly suppressed also at the kilovoltage energy level. Conversely, MLDR (6 MV) exerted minimal effects and did not produce statistically significant improvements. Taken together, our findings demonstrate that radiation energy level is a key determinant of LDR therapeutic efficacy in AD mice, with KLDR showing significantly greater effectiveness in improving AD-related pathological features than MLDR. Therefore, KLDR may be recommended as a novel radiation protocol for AD treatment.

Keywords: Alzheimer's disease; low-dose radiation; kilovoltage energy; amyloid-β; tau

1. Introduction

Low-dose radiation (LDR) therapy attracts public attention with the accumulating evidence for radiation hormesis [1]. Over the past few decades, a great deal of effort has been made to verify the efficacy of LDR in both normal and pathological conditions, finding that LDR plays a key role in triggering multiple adaptive responses in organisms to protect them against endo- and exogenous health threats [2–4]. Specifically, regarding transcriptomic analysis, there were two pioneering

 doi:10.20944/preprints202604.0063.v1

experiments to assess alterations in gene expression after LDR. Yin et al. reported that 0.1-Gy radiation positively regulated genes engaged in protective and reparative functions in mouse brains, including stress response and DNA synthesis/repair [5]. Lowe et al. showed that 0.1-Gy radiation downregulated cognitive dysfunction-associated neural pathways, and conversely, at a higher dose (2 Gy), any of the pathways were not elicited. Accordingly, the authors proposed that LDR at 0.1 Gy may exert beneficial effects on cognitive function [6]. These results provided a crucial clue that LDR might be used as an alternative modality for improving cognitive decline.

Meanwhile, a previous case-based analysis reported a notable finding: orthovoltage X-rays (typically 150–500 kV) were superior to linear accelerator-based radiotherapy (6 or 10 MV) for the treatment of osteoarthritis. Based on an analysis of 9,802 patients reported in the literature, significant clinical benefits of orthovoltage radiotherapy were observed in terms of both complete and partial responses [7]. These findings underscore the significance of radiation energy levels in treating inflammatory and neurodegenerative diseases.

More recently, Kim et al. reported novel findings elucidating part of the mechanism underlying LDR-induced cognitive improvement. They demonstrated LDR-induced microglial polarization from M1 to M2, which in turn upregulated anti-inflammatory cytokines and ultimately mitigated neuroinflammation in AD mice [8]. These results offered rational evidence of how LDR ameliorates inflammatory milieus in AD brains [9,10]. Furthermore, LDR exerted direct neuroprotective effects by promoting cell viability and reducing DNA fragmentation against β-amyloid (Aβ) toxicity [11]. Clinical studies supported these results, reporting that LDR showed slight or meaningful improvements in early-to-advanced AD patients along with a positive safety profile [12–14]. However, the central question of what radiation energy range LDR is most effective for AD treatment has not yet been fully addressed.

Accordingly, the present study conducted a direct comparative evaluation on the efficacy of LDR at two different energy levels—kilovoltage and megavoltage—with respect to improvements in AD pathological features such as inflammation, Aβ/tau burden, neuronal degeneration, and cognitive decline. Eventually, we tried to provide reliable interpretations and rationales for KLDR, suggesting a novel therapeutic approach for AD. This is the first study of its kind.

2. Results

2.1. A Marked Inhibition of Cognitive Decline at Kilovoltage, but not Megavoltage, Energy

In accordance with the radiation protocol and study timeline, MLDR or KLDR was delivered to the brains of AD mice over 2.5 weeks, and then pre- and post-treatment evaluations were carried out using behavioral, histological, and molecular analysis methods (Figure 1A,B).

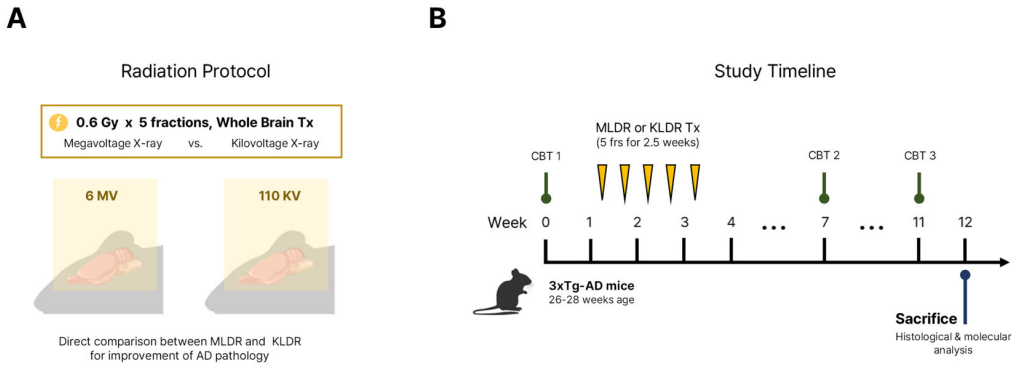

Figure 1. X-ray irradiation protocols (A) and experimental schedules (B) were summarized. Whole-brain MLDR or KLDR treatments (0.6 Gy × 5 fractions) were performed in 3xTg-AD mice. Pre- and post-treatment assessments were conducted to evaluate LDR efficacy under two distinct radiation protocols (KLDR vs. MLDR; A–B). Tx, treatment; frs, fractions.

 doi:10.20944/preprints202604.0063.v1

Latency (sec) during the acquisition (A) and retention (R) phases was measured at each time point (Figure 2A–C). The latency difference (R-A) served as an index of memory performance. At baseline (Week 0), the latency difference indicated no significant differences between groups (Figure 2A). Post-treatment, mice in the KLDR group demonstrated significantly delayed entry into the dark chamber compared to sham at Week 7 and Week 12 (both, $p<0.01$; Figure 2B,C). In addition, NOR tests indicated enhanced exploratory trajectories around the novel object (blue circle) in the treatment groups (Figure 2D), with PI and DI significantly higher in KLDR mice compared to sham at Week 12 (both, $p<0.05$; Figure 2E,F). In contrast, MLDR treatment produced no significant changes in both tests (Figure 2B,C,E,F). All values were summarized in Supplementary Table S1.

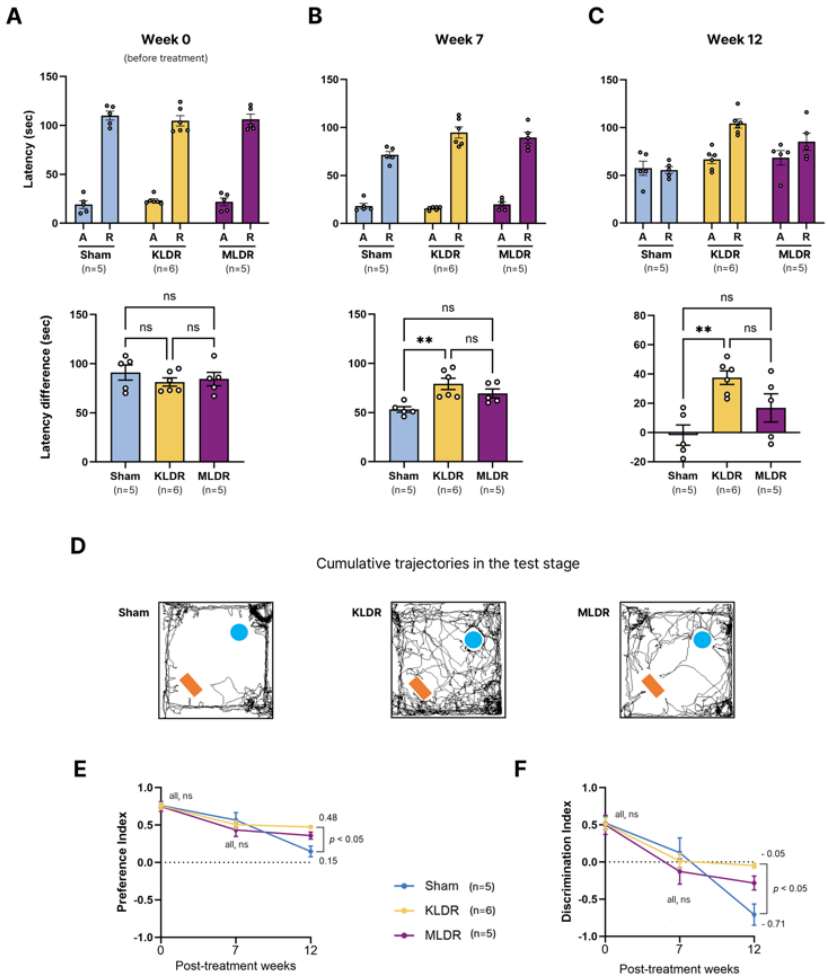

Figure 2. In the PA test, comparable performance was observed among groups at baseline (A). KLDR-treated mice showed significantly increased latency at Weeks 7 and 12 compared to the sham control (both, $p<0.01$), while MLDR had minimal effects (B, C). In the NOR test, cumulative movement trajectories of all mice during the test stage were visualized (D). KLDR mitigated the decline in object interest observed in sham mice, as evidenced by higher PI (E) and DI (F) values at Week 12 (both, $p<0.05$). MLDR effects remained negligible across assessments (E, F). *, ** denote statistical significance at $p<0.05$ and $p<0.01$, respectively. NS, not significant.

2.2. A Marked Reduction in Inflammatory Marker Levels at Kilovoltage, but not Megavoltage, Energy

To examine changes in the brain microenvironment after treatment, we first investigated the increase or decrease in the expression level of inflammatory markers. Co-immunostaining experiments revealed reduced Iba-1 and GFAP expressions in the hippocampal CA1 (Figure 3A) and dSub (Figure 3B) regions after treatment. KLDR treatment markedly decreased Iba1-positive and GFAP-positive cell counts in both regions compared to the sham control (Iba-1, $p<0.001$; GFAP, $p<0.01$; Figure 3C–F). Conversely, MLDR did not induce significant changes and exhibited markedly

 doi:10.20944/preprints202604.0063.v1

lower efficacy compared to KLDR (Iba-1 CA1, $p<0.001$; Iba-1 dSub, $p<0.01$; GFAP both regions, $p<0.05$; Figure 3C–3F). In addition, hippocampal TNF-α and IL-6 levels were much downregulated in the KLDR group, whereas neither of the MLDR groups showed any meaningful alterations (Supplementary Figure S1). All values were summarized in Supplementary Table S2.

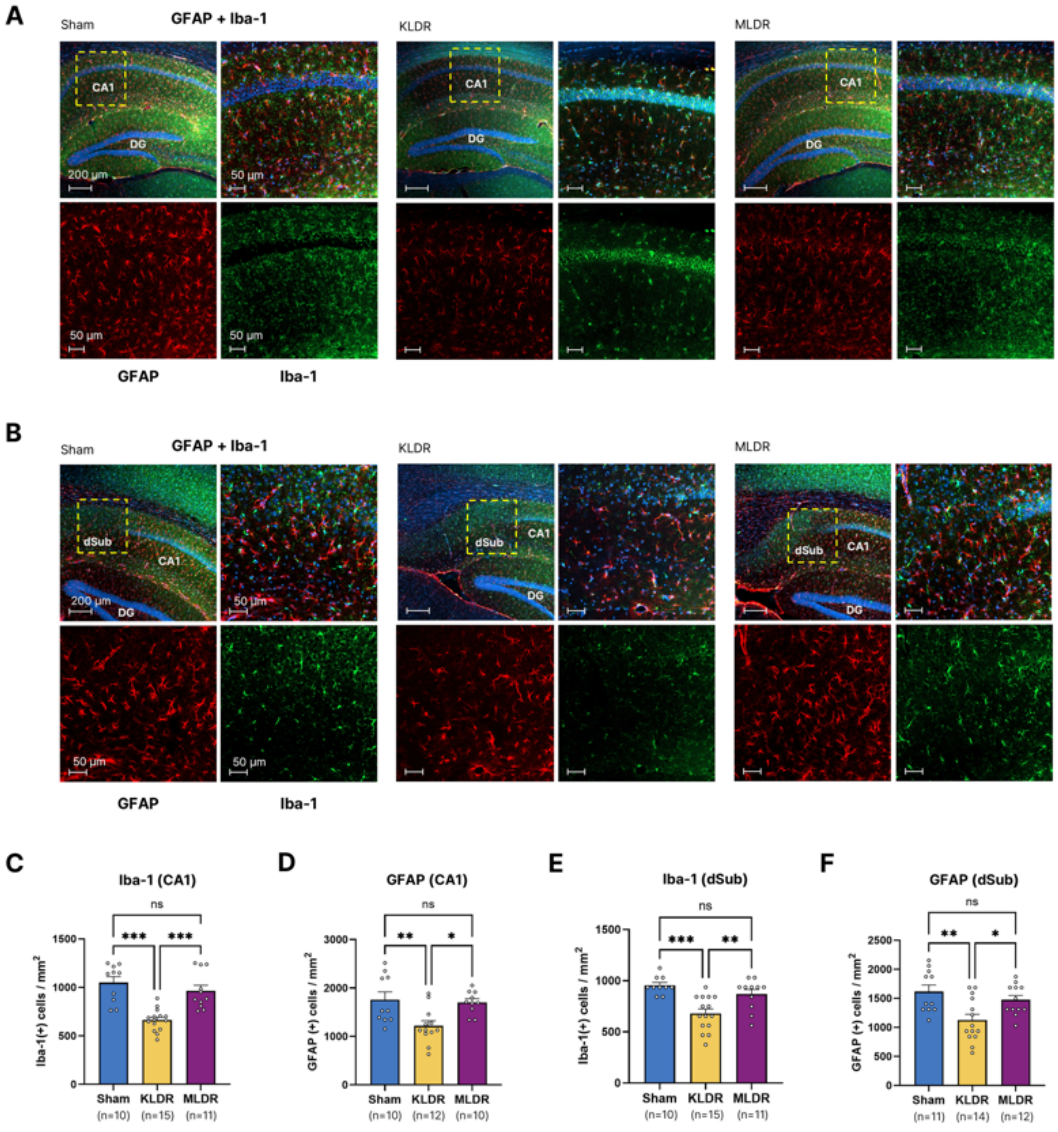

Figure 3. Inflammatory markers, Iba-1 and GFAP, were co-stained in hippocampal slices (A, B). Significant reductions in their levels were observed in the CA1 (C, D) as well as the dSub (E, F) regions between the KLDR and sham groups (Iba-1: $p<0.001$; GFAP: $p<0.01$). In contrast, the MLDR regimen demonstrated minimal impact across regions, exhibiting substantially lower anti-inflammatory effects compared to KLDR ($p<0.05$, $p<0.01$, $p<0.001$; C–F). Two to three brain tissue slices were used per mouse. *, **, and *** denote statistical significance at $p<0.05$, $p<0.01$, and $p<0.001$, respectively. NS, not significant.

2.3. A Marked Reduction in Aβ Deposition at Kilovoltage, but not Megavoltage, Energy

It is well established that Aβ is a critical initiator that greatly affects AD progression via plaque formation. The 4G8 antibody was used to stain Aβ plaques and quantify their intensity in hippocampal slices (Figure 4A), finding that Aβ plaque intensity was greatly reduced in the KLDR group (vs. sham, $p<0.05$; Figure 4C left panel). There was also a drop in the intensity in the MLDR group, which, however, was not statistically significant. Thioflavin S was used to detect Aβ plaques, confirming the reproducibility of the above findings (sham vs. KLDR, $p<0.05$; Figure 4B,C right

 doi:10.20944/preprints202604.0063.v1

panel). In addition, intracellular Aβ deposition in the amygdala and cortical slices was examined by quantifying 6E10 antibody immunoreactivity. KLDR exerted a pronounced effect in reducing the number of 6E10-positive cells in the slices, whereas MLDR did not elicit these responses (Supplementary Figures S2 and S3).

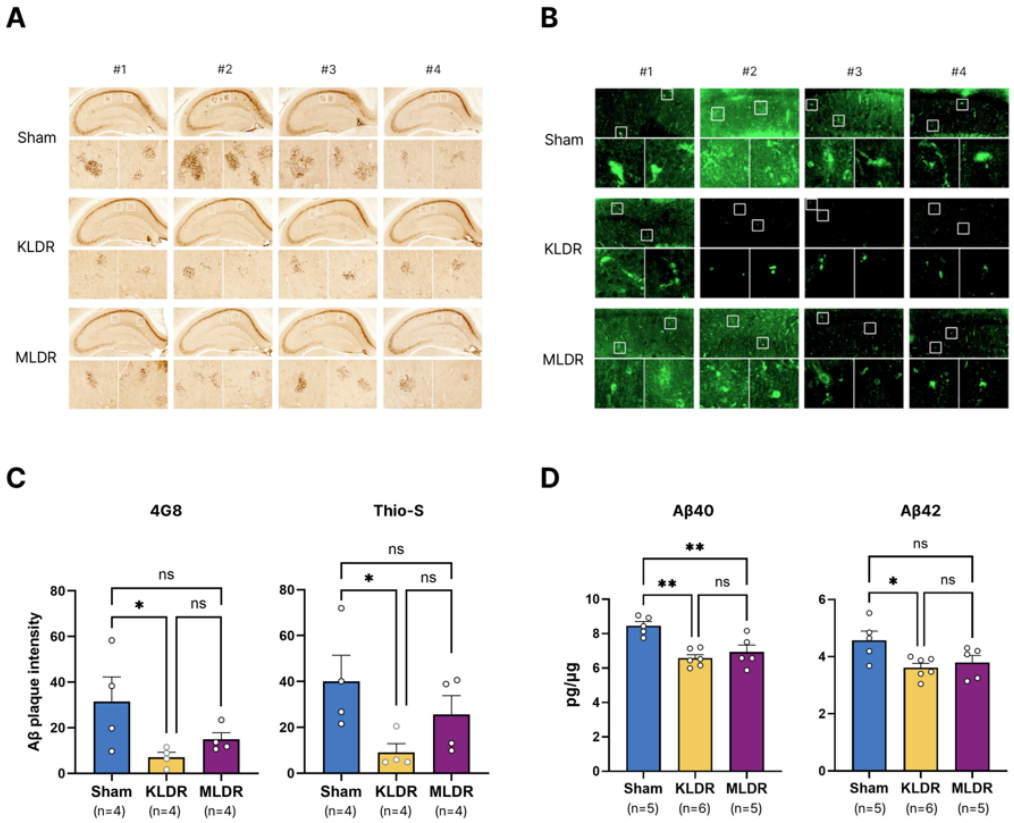

Figure 4. 4G8 and Thioflavin S analyses were conducted to assess extracellular Aβ burden in the hippocampus (A, B), showing a significant reduction in Aβ plaque intensity in the KLDR group (vs. sham, $p<0.05$), while MLDR showed no significant effects in either assay (C). In addition, Aβ40 levels were much reduced in both treatment groups (vs. sham, $p<0.01$; D left panel). However, a significant reduction in pathogenic Aβ42 levels was observed exclusively in the KLDR group (vs. sham, $p<0.05$; D right panel). * and ** denote statistical significance at $p<0.05$ and $p<0.01$, respectively. NS, not significant.

Next, Aβ40 and Aβ42 levels were separately quantified using the ELISA technique in the hippocampus of AD mice. Notably, Aβ42 is known to greatly contribute to Aβ plaque formation. Aβ40 levels were significantly reduced in both KLDR and MLDR groups (vs. sham, $p<0.01$; Figure 4D left panel). Notably, a significant reduction in Aβ42 levels was observed exclusively in the KLDR group (vs. sham, $p<0.05$). A decreasing trend was observed in the MLDR group, but it did not reach statistical significance (Figure 4D right panel). Collectively, KLDR effectively alleviated Aβ burden in both intra- and extracellular regions, whereas MLDR exhibited only minor reductions. All values were summarized in Supplementary Table S3.

2.4. A Marked Reduction in Tau Deposition at Kilovoltage, but not Megavoltage, Energy

Tau is another critical pathogenic protein in AD. Under AD conditions, tau undergoes abnormal phosphorylation, leading to its aggregation into neurofibrillary tangles. In this experiment, tau markers including HT7 (for total tau) and AT180 (for phospho-tau) were identified, and their expression levels were quantified in the hippocampal region of AD mice (Figure 5A–D).

 doi:10.20944/preprints202604.0063.v1

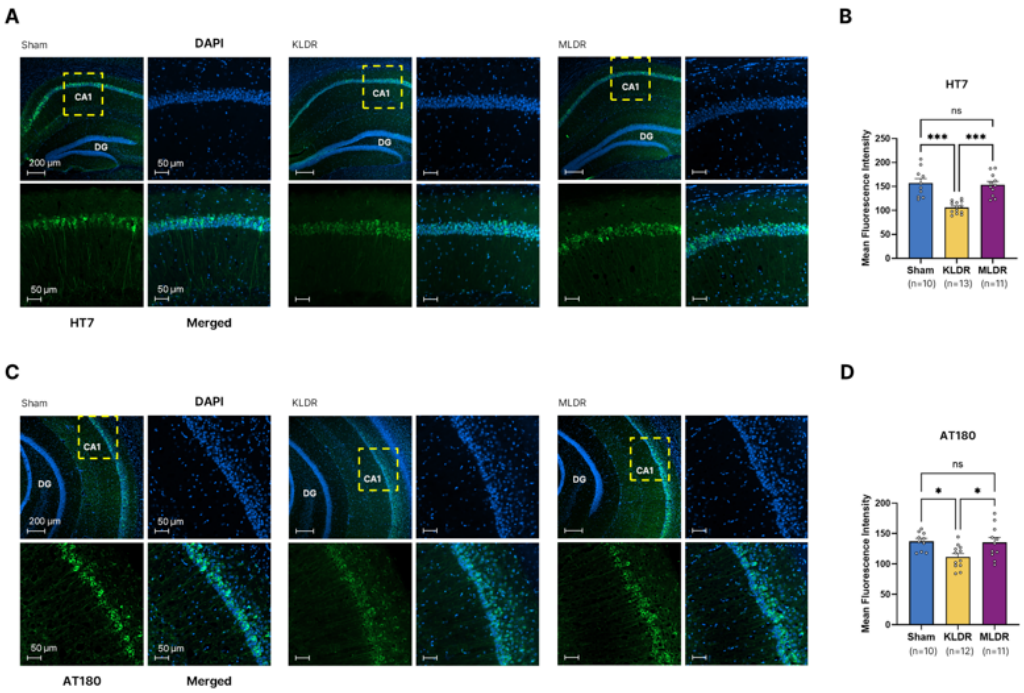

Figure 5. The HT7 (tau) and AT180 (p-tau) levels were visualized in the CA1 region of AD mice (A, C). The levels of both markers in hippocampal slices were significantly reduced in the KLDR group (vs. sham, $p<0.001$ or $p<0.05$; B, D). Notably, the KLDR regimen exerted a substantially stronger effect in reducing tau levels compared to MLDR ($p<0.05$, $p<0.01$; B, D). Two to three brain tissue slices were used per mouse. *, **, and *** denote statistical significance at $p<0.05$, $p<0.01$, and $p<0.001$, respectively. NS, not significant.

Histological analysis revealed a significant reduction in the fluorescence intensity of HT7 in the KLDR group (vs. sham, $p<0.001$; Figure 5A,B). Likewise, the intensity of AT180 was also markedly decreased in the KLDR group (vs. sham, $p<0.05$; Figure 5C,D). In contrast, the MLDR group showed no significant reductions in both HT7 and AT180 levels and demonstrated significantly lower efficacy compared to the KLDR group (HT7, $p<0.001$; AT180, $p<0.05$; Figure 5B,D). However, MLDR failed to induce these alterations, resulting in minimal reduction of tau burden (Figure 5A–D).

2.5. Significant Inhibition of Neuronal and Synaptic Degeneration at Kilovoltage, but not megavoltage, Energy

Finally, changes in neuronal and synaptic degeneration were examined by quantifying neurons (NeuN) and synaptic function (SYN) markers after KLDR or MLDR treatment. In effect, these two factors are considered to directly impact on cognitive function. NeuN-positive cell counts were measured in the dSub region, but in the CA1 region, NeuN fluorescent intensity was quantified instead of cell counting due to extensive cellular overlap in that area. NeuN fluorescent intensity was significantly increased in the KLDR group (vs. sham, $p<0.05$ for CA1; Figure 6A,B). Furthermore, the number of NeuN-positive cells was markedly elevated in the KLDR group (vs. sham, $p<0.01$ for dSub; Figure 6C,D). Similarly, SYN levels in the CA1 and dentate gyrus (DG) regions were significantly increased in the KLDR group (vs. sham, $p<0.001$ for CA1, $p<0.01$ for DG; Figure 6E–G). In contrast, MLDR failed to induce these alterations. Furthermore, significant differences were observed between the KLDR and MLDR groups ($p<0.05$, $p<0.001$), indicating that MLDR exerted minimal effects (Figure 6A–G). All values were summarized in Supplementary Table S5.

 doi:10.20944/preprints202604.0063.v1

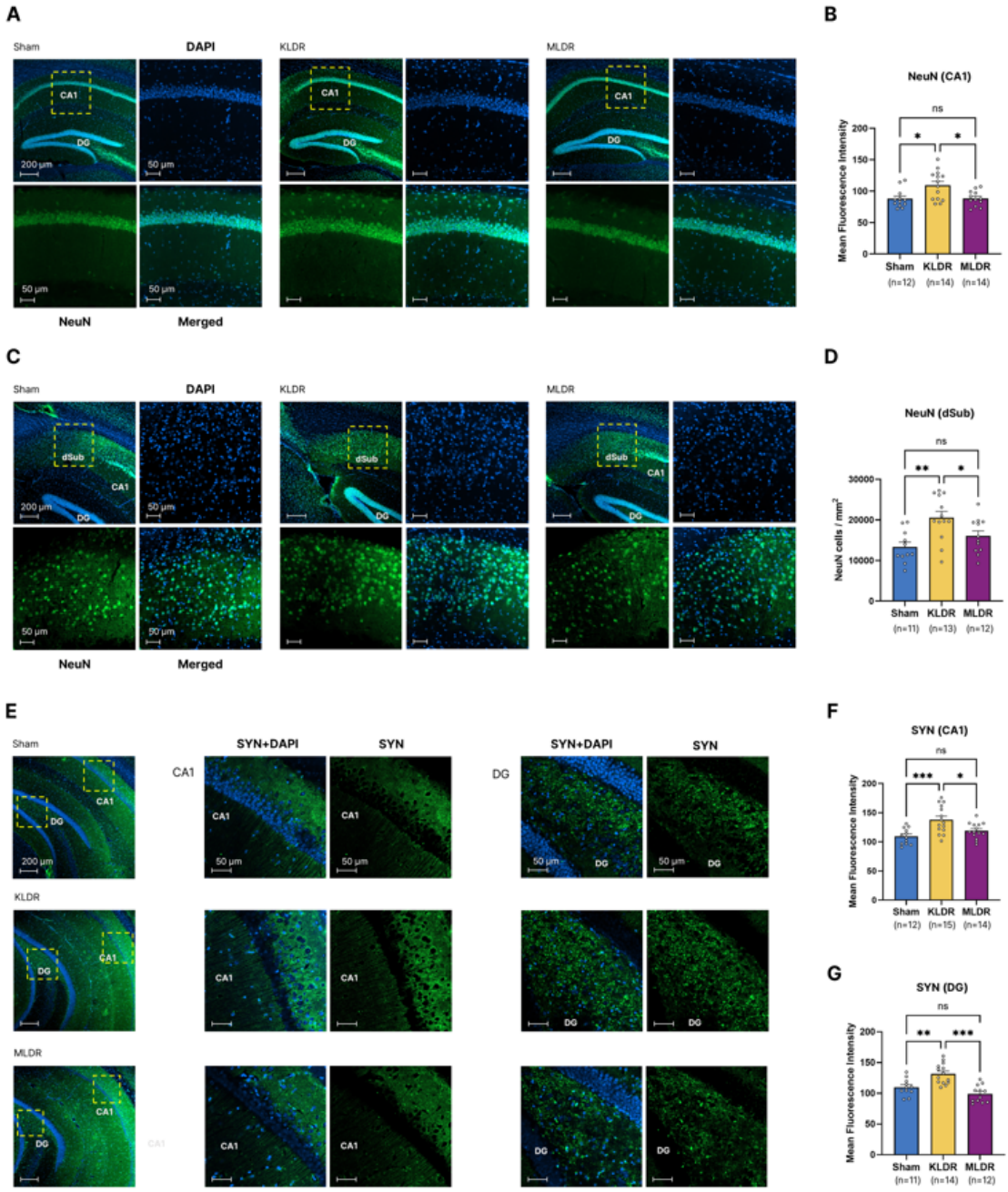

Figure 6. NeuN levels were visualized in the CA1 and dSub regions (A, C), and were significantly increased in the KLDR group (vs. sham, $p<0.05$ or $p<0.01$; B, D). In addition, SYN levels were visualized in the CA1 and DG regions (E), and were significantly increased in the KLDR group (vs. sham, $p<0.001$ or $p<0.01$; F, G). In contrast, the MLDR regimen exerted only minimal effects. Importantly, the KLDR regimen exerted a substantially stronger effect in inhibiting neuronal and synaptic degeneration (vs. MLDR, $p<0.05$ or $p<0.001$; B, D, F, G). Two to three brain tissue slices were used per mouse. *, **, and *** denote statistical significance at $p<0.05$, $p<0.01$, and $p<0.001$, respectively. NS, not significant.

2.6. KLDR Shows Multimodal Actions, Improving Typical AD Pathological Features

All the experiments and results are schematically presented in Figure 7. Low-dose X-rays were applied to the brains of AD mice at the kilovoltage and megavoltage energy ranges. Cognitive decline was markedly suppressed in the KLDR group. Pronounced anti-inflammatory and neuroprotective effects were also observed at the kilovoltage energy level. Notably, in terms of Aβ and tau burden, mice in the KLDR group exhibited a significant reduction compared to the sham control. In contrast,

 doi:10.20944/preprints202604.0063.v1

at the megavoltage energy level, a trend toward improvement of AD pathological features was observed, although it was not statistically significant.

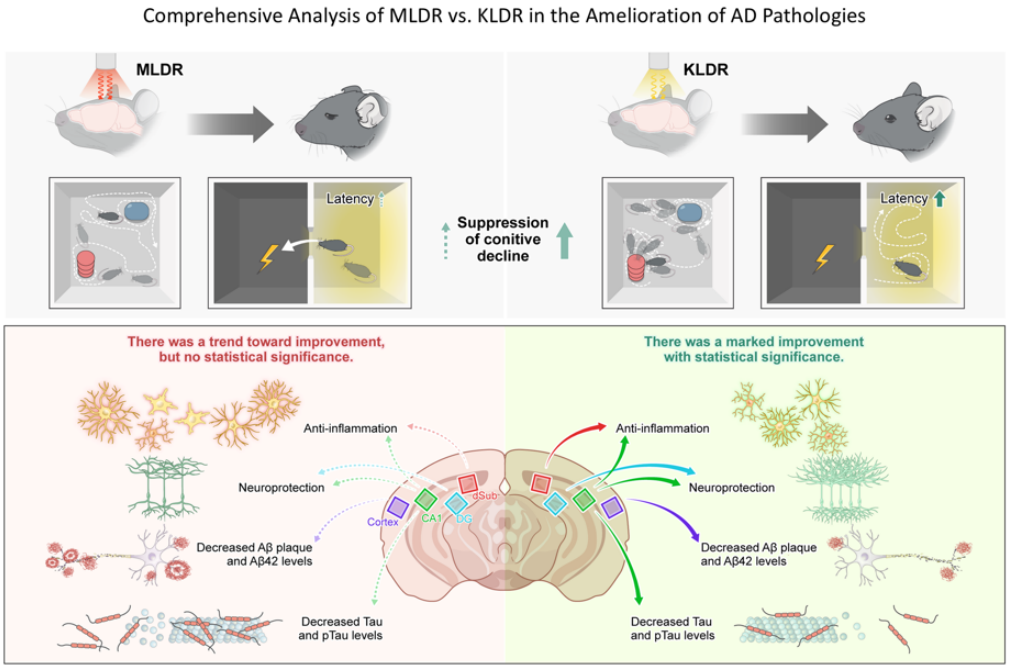

Figure 7. All findings, ranging from cognitive behavioral tests to histological and molecular examinations, are illustrated. Notably, KLDR demonstrated significant improvements in key AD pathological features examined in this study, whereas MLDR exhibited a trend toward improvement that did not reach statistical significance.

3. Discussion

The present study revealed that LDR exerted differential effects in AD mice depending on the radiation energy level. Specifically, KLDR exerted multimodal actions that markedly alleviated inflammation, intra- and extracellular Aβ accumulation, tau burden, and neuronal and synaptic degeneration in key brain regions involved in cognitive function—namely, hippocampal regions (CA1, DG, dSub), cortex, and amygdala—ultimately leading to a significant suppression of cognitive decline in AD mice. In contrast, the MLDR regimen exerted only minimal effects on ameliorating these AD pathological features.

Emerging evidence identifies low-energy irradiation as a critical factor in enhancing therapeutic outcomes for neurodegenerative diseases under LDR protocols. Orthovoltage X-rays have demonstrated superior efficacy over megavoltage beams in treating degenerative joint diseases [7]. In addition, Ceyzériat et al. applied 2-Gy 4-MV X-rays to AD mice over five sessions via a linear accelerator; however, this protocol did not significantly reduce Aβ deposition [15]. Subsequently, they conducted another LDR study using 100 kV X-rays with the same 5×2 Gy doses, which significantly reduced Aβ deposition [16]. These findings indicate that LDR efficacy depends on its energy level, with KLDR showing greater therapeutic effects than MLDR in AD mice.

Neuroinflammation is a common feature of neurodegenerative diseases, having a profound effect on their pathogenesis [17,18]. Importantly, our study found that KLDR has a key role in improving AD-induced inflammatory milieus by markedly mitigating the level of pro-inflammatory cytokines and astrocytes. Previous studies demonstrated that KLDR could modulate innate immune system by inducing microglial polarization into the M2 profile against lipopolysaccharide (LPS)-induced inflammation, thus suppressing the production of pro-inflammatory cytokines and encouraging that of anti-inflammatory ones [8]. This can be a possible mechanism of how KLDR lessens the production of pro-inflammatory cytokines.

 doi:10.20944/preprints202604.0063.v1

In addition, KLDR-induced downregulation of pro-inflammatory cytokines are connected with the reduction in Aβ and tau burden. A previous study showed that interferon-induced transmembrane protein 3 (IFITM3) played a pivotal role in producing Aβ40 and Aβ42 by forming a complex with γ-secretase [19]. Interestingly, IFITM3 expression was governed by pro-inflammatory cytokine levels. In other words, these cytokines positively modulated IFITM3 expression, which in turn increased Aβ production [20,21]. Son et al. reported that 0.1 or 0.3-Gy radiation induced a decrease in IFITM3 expression and then relieved Aβ burden [22]. Meanwhile, it is well established that increased Aβ burden or increased inflammatory responses lead to worsening tau pathology [23,24]. Thus, the KLDR-induced downregulation of pro-inflammatory cytokines is deeply associated with reduction in tau burden. Taken together, it can be speculated that KLDR-induced suppression of pro-inflammatory cytokines leads to reduced IFITM3 expression, which in turn decreases Aβ and tau burden.

It is generally accepted that Aβ deposition is one of the most representative pathological phenotypes for AD [25,26]. The Aβ fibrils augment oxidative stress and trigger inflammatory cascade, in turn accelerating cell death and causing fatal damage even to nearby neurons [27]. Interestingly, Aβ accumulates in both intracellular and extracellular spaces. A great body of evidence revealed that intracellular Aβ was produced within the endoplasmic reticulum (ER) and Golgi system or was derived from internalized extracellular Aβ [28,29]. In this regard, to relieve the entire burden of Aβ peptides, it is crucial to diminish both intra- and extracellular Aβ deposition and thereby minimize cellulogenic risk factors. Our study showed that there was a marked alleviation in Aβ deposition in both intra- and extracellular areas after KLDR treatment. It suggests that KLDR has a key role in improving intra- and extracellular Aβ burden in AD brain.

Then, a question remains about why such effects are induced under KLDR, rather than MLDR, regimen. A previous study explained that orthovoltage radiation exhibits higher X-ray absorption in tissues, along with more pronounced anti-inflammatory effects in surrounding organs [7]. Basically, photoelectric effects predominate at the relatively low X-ray energy range, indicating that the probability of photoelectric absorption decreases with increasing radiation energy [30,31]. These results imply that low-energy X-rays are more likely to induce biological effects in the targeted tissue than high-energy ones. Specifically, Amols et al. reported that at doses of 100-rad (1 Gy) or less, megavoltage photons (or electrons) showed radiobiological effectiveness (RBE) less than 0.8 compared to orthovoltage X-rays, and which might decrease significantly at lower doses. It indicates that the RBE of orthovoltage X-rays is at least 20% greater than that of the megavoltage radiation at 1-Gy dose or less [32].

In the present study, we employed the 3xTg-AD mouse model, which recapitulates both amyloid-β and tau pathology and reflects key features of AD. Its age-dependent progression enables evaluation of low-dose radiation therapy (LDRT) effects across disease stages, including amyloid deposition, tau pathology, neuroinflammation, and synaptic function [33]. However, as a familial AD–based model with relatively slow plaque development, it may not fully represent sporadic AD and can require longer experimental timelines [34]. Despite these limitations, it remains a valuable platform for integrated assessment of therapeutic effects. The AD mice used in this study were 26–28 weeks old, an age at which neuroinflammation and Aβ/tau pathology begin to manifest [35], reflecting early-stage AD in clinical settings. At this stage, extracellular Aβ42 deposition forms amyloid plaques, while phosphorylated tau accumulates within neurons. Early microglial and astrocytic activation contributes to neuronal damage, synaptic loss, and subsequent cognitive decline [36] [37]. In this study, we analyzed each of the factors as a function of radiation energy level and demonstrated the therapeutic efficacy of low-energy LDR (KLDR) in this disease process.

Notably, our outcomes were achieved using a substantially lower radiation dose (0.6 Gy per fraction; total dose of 3 Gy) compared to that used in previous radiation studies (typically 2 Gy per fraction; total dose of 10 Gy), representing an approximately threefold reduction [8,11,14–16,38–42]. This difference highlights that therapeutic effects can be attained even at markedly reduced dose levels. In particular, our results suggest that modulation of AD pathology does not necessarily require

 doi:10.20944/preprints202604.0063.v1

higher radiation exposure, but may instead depend on appropriately optimized irradiation conditions, including energy and dose rate. From a translational perspective, the use of lower doses may also help minimize potential radiation-related risks while maintaining efficacy. These findings indicate that AD pathology can be improved at lower radiation doses, offering valuable evidence for optimizing LDR regimens. Therefore, these results provide important evidence that AD pathology can be improved at lower radiation doses and support the optimization of LDR regimens toward safer and more clinically feasible therapeutic strategies.

The radiation dose (Gy) applied in this study was determined through a combination of literature review and experimental validation. In a pioneering approach, a 2-Gy protocol (2 Gy per fraction × 5; total dose, 10 Gy) was adopted in LDRT studies for AD mice [40,43]. Yang et al. evaluated both the 2-Gy protocol and a 0.6-Gy protocol (0.6 Gy per fraction × 5; total dose, 3 Gy) in AD mice, demonstrating that the 0.6-Gy protocol produced therapeutic effects comparable to those of the 2-Gy protocol [42]. Subsequently, the 0.6-Gy protocol has been applied not only to AD [44] but also to other conditions, including osteoarthritis [45]. Based on these prior findings, together with our experimental validation, we determined that the 0.6-Gy protocol is appropriate for the present study.

KLDR irradiation is technically feasible for the human brain, despite the presence of cranial bone. The mass attenuation coefficients (μ/ϱ, m^2/kg) of 100 keV X-ray photon energy in water and bone are 1.707×10^{-2} and 1.855×10^{-2}, respectively, indicating a maximum difference of approximately 8.76% at best [46]. This discrepancy is further reduced when 110 keV X-rays—slightly exceeding 100 keV—are utilized. Given an average skull thickness of 6.9 mm (range: 6.5–7.1 mm) [47], exponential attenuation analysis ($I = I_0 \cdot e^{-\mu x}$) indicates ~78.9% X-ray transmission, supporting sufficient energy delivery to the brain during whole-brain LDR in humans.

Lastly, this study was conducted using male mice. Generally, in 3xTg-AD mice, females exhibit more severe disease progression in terms of Aβ/tau pathology and neuroinflammation compared to males [35]. Likewise, lecanemab—a newly approved drug for Alzheimer's disease (AD)—has shown limited efficacy in female patients [48]. Given these sex-dependent differences in disease progression and severity, we considered that mixing male and female mice within the same experimental group could introduce substantial biological variability. Accordingly, the present study focused on male mice to ensure experimental consistency and reduce potential confounding effects. In future studies, we plan to systematically investigate whether the therapeutic efficacy of LDRT differs between sexes or remains consistent regardless of sex, thereby addressing sex-specific responses to LDRT.

4. Materials and Methods

4.1. Animals and Group Assignment

A total of 16 male homozygous 3xTg-AD transgenic mice [B6;129-Tg(APPSwe,tauP301L)1Lfa *Psen1*^{tm1Mpm}/Mmjax] (Jackson Laboratory, Bar Harbor, ME, USA) aged 26-28 weeks old were used in the study. All mice were housed 4 to 5 per cage at room temperature with an alternating 12/12 h light/dark cycle and free access to food and water. They were assigned to the following groups: Sham (n=5), KLDR (n=6), and megavoltage LDR (MLDR, n=5) groups. Sham radiation is defined by a radiation regime in which LDR is irradiated with 0 Gy dose in each treatment.

4.2. Cranial LDR Procedure

Mice were anesthetized with an intraperitoneal injection of Zoletil (2.5 mg/kg, Virbac, Carros, France) using a 0.5 mL insulin syringe with an ultra-fine needle (BD Biosciences, San Jose, CA, USA) and were placed on an immobilizer before irradiation. The head irradiation was performed at a dose of 0.6 Gy twice a week for two and a half weeks, a total of 5 times (total dose, 3 Gy in 5 fractions), using an in vivo X-ray irradiation system (RS320, Xstrahl Ltd., UK) for the KLDR group (110 kV, 10 mA, 0.6 Gy/min), or a linear accelerator (RapidArc, Varian Medical Systems, Palo Alto, USA) for the MLDR group (6 MV, 0.6 Gy/min). In the sham group, all procedures were conducted identically to those in the LDR treatment groups (KLDR and MLDR), except that irradiation was delivered at 0 Gy.

 doi:10.20944/preprints202604.0063.v1

4.3. Cognitive Behavioral Tests

4.3.1. Passive Avoidance (PA) Test

The passive avoidance test was performed using a test apparatus (LE872, Panlab, Spain): 250 (W) x 250 (D) x 240 (H) mm white compartment and 195 x 108 x 120 mm black compartment. For adaptation training, the animals were placed in the light compartment for 10 min and allowed to freely enter and exit both compartments for 10 min. On the training day, each mouse was allowed to move freely into the dark chamber, where then the mouse was given 0.3 mA electrical shock in 5 seconds. On the next day, the mice were re-tested in the same way, and the step-through latency before re-entering the dark side was measured up to 300 seconds using SHUTAVOID software (Panlab, Spain).

4.3.2. Novel Object Recognition (NOR) Test

Mice were first acclimated to a 45 cm cube-shaped test chamber on Day 1. The following day, they were exposed to two identical objects within the same environment to facilitate object familiarization through free exploration. Subsequently, one of the objects was replaced with a novel object. All behavior of the mice inside the chamber was video recorded. The trajectories of object exploration were analyzed with a SMART video tracking S/W (PanLab Harvard Apparatus, MA, USA). The Preference Index (PI) and Discrimination Index (DI) were used for quantifying the interest of AD mice in the novel object. The formulas of the indices are: PI, Time spent on novel object / Time spent on novel object + Time spent on familiar; DI, Time spent on novel object—Time spent on familiar object / Time spent on novel object + Time spent on familiar.

4.4. Brain Tissue Preparation

AD mice were sacrificed under isoflurane inhalation anesthesia (2.0–2.5% v/v in O2) using an isoflurane vaporizer (VetEquip, Livermore, CA, USA) at 9 weeks after the last treatment. They were transcardially perfused with phosphate-buffered saline (PBS) and brains were carefully dissected. The extracted brains were sagittally divided in half. One half was used for histological analysis, and the other half was used for mRNA or protein quantification. Each brain section was prepared in the horizontal plane at a thickness of 40 μm using a microtome (Leica VT1000S, Nussloch, Germany). In histological analyses, one or 2-3 brain slice tissues were used per mouse. Histological and quantitative analyses were performed in key brain areas closely related to cognitive function such as hippocampus [CA1, dorsal subiculum (dSub), dentate gyrus], corte—x, and amygdala.

4.5. Histological Analyses

4.5.1. Immunofluorescence Analysis

Free-floating brain sections were incubated overnight at 4 °C with the following primary antibodies: rat monoclonal glial fibrillary acidic protein (GFAP) (1:1000; 13-0300, Thermo Fisher Scientific Inc.), goat polyclonal ionized calcium binding adaptor molecule 1(Iba-1) (1:250; ab5076, Abcam), mouse monoclonal neuronal nuclei (NeuN) (1:100; MAB377, Sigma-Aldrich), mouse synaptophysin (SYN) (1:500; S5768, Sigma-Aldrich), mouse monoclonal Tau (HT7) (1:1000; MN1000, Thermo Fisher Scientific Inc.), mouse monoclonal phospho-Tau (AT180) (1:500, MN1040, Thermo Fisher Scientific Inc.). Subsequently, Alexa Fluor-conjugated secondary antibodies were applied for 1 hour at room temperature. Stained sections were mounted and imaged using a slide scanner (Axio Scan, Carl Zeiss).

4.5.2. Immunohistochemical Analysis

For anti-6E10 and anti-4G8 staining, the sections were incubated at 4 °C on a shaker overnight with the following primary antibodies: mouse monoclonal β-Amyloid (6E10; 1:200; 803001,

 doi:10.20944/preprints202604.0063.v1

Biolegend) (4G8; 1:200; 800701, Biolegend). Afterwards, the sections were incubated with #4 Linking Reagent and #5 Labeling Reagent for 20 min each on a shaker at room temperature (929501, Biolegend), and then mounted on slides. All stained sections were photographed under a microscope slide scanner (Axio scan, Carl Zeiss).

4.5.3. Thioflavin S Staining

Free-floating sections were left to air dry overnight at room temperature and were then incubated for 10 min in 1% Thio-S (T1892, Sigma-Aldrich). After washed in 70% and 50% alcohol and then in distilled water, the sections were mounted on slides. All stained sections were photographed under a microscope slide scanner (Axio scan, Carl Zeiss).

4.6. Quantitative Molecular Analyses

4.6.1. Quantitative Real-Time Reverse-Transcription PCR (qRT-PCR)

cDNA synthesis was accomplished using 1 μg of isolated RNA and ReverTra Ace™ qPCR RT Master Mix (FSQ-201, TOYOBO). qRT-PCR was performed using 2X Fast Q-PCR Master Mix (TQ1210, SMOBIO). The following sets of sense/antisense primers were used: (i) F, 5′-GAGGATACCACTCCCAACAGACC-3′ and R, 5′-AAGTGCATCATCGTTGTTCATACA-3′ for Interleukin 6 (IL-6); (ii) F, 5′-TCGTAGCAAACCACCAAGTG-3′ and R, 5′-ATATAGCAAATCGGCTGACG-3′ for Tumor necrosis factor alpha (TNF-α); (iii) F, 5′-TGGCACAGTCAAGGCTGAGA-3′ and R, 5′-CTTCTGAGTGGCAGTGATGG-3′ for GAPDH. Gene expression analysis was realized in a CFX Connect Real-Time PCR Detection System (1855201, Bio-Rad), and the data were analyzed by CFX Maestro Software (Bio-Rad).

4.6.2. Enzyme-Linked Immunosorbent Assay (ELISA)

Quantification of Aβ42 and Aβ40 was performed using commercially available sandwich ELISA kits (R&D Systems, Minneapolis, MN, USA). Briefly, Samples and standards were assayed using 96-well plates coated with monoclonal antibodies specific to Aβ42 or Aβ40. Detection involved biotinylated antibodies, HRP-conjugated streptavidin, and TMB substrate. Absorbance at 450 nm was measured using a microplate reader (Molecular Devices, SpectraMax plus 384), and concentrations were determined from standard curves.

4.7. Statistical Analysis

Statistical analyses were conducted using GraphPad Prism 10.2.3 (GraphPad Software Inc. San Diego, CA, USA) and SPSS software ver. 26 (IBM, Armonk, NY, USA). Data produced in the study were represented as mean ± standard errors of mean (SEM). Differences between groups were analyzed using a one-way repeated measures analysis of variance (ANOVA), followed by a post hoc Tukey's test or Holm-Sidak for multiple comparisons. Data, which were not evenly distributed and did not pass the normality test, were analyzed using the Friedman test with a post hoc Tukey's test for multiple comparisons. P values of less than 0.05 were considered statistically significant.

5. Conclusions

This study is the first direct comparative evaluation of KLDR and MLDR in AD mice, focusing on the amelioration of early-stage AD features. Our findings suggest that kilovoltage energy is a key factor of LDR efficacy and support KLDR as a promising approach for AD treatment. Further studies are warranted to fine-tune this regimen and advance toward an optimized therapeutic protocol. Notably, variations in dose rate can lead to distinct biological outcomes, and identifying the optimal dose rate for improving AD remains an important research challenge. In general, lower dose rates allow more time for the repair of DNA damage and cellular injury [49]. Importantly, these findings provide a translational basis for the clinical application of KLDR, as kilovoltage X-ray systems are

 doi:10.20944/preprints202604.0063.v1

widely available and may allow safe and precise dose delivery in clinical settings. With further validation in large-animal models and well-designed clinical studies, KLDR could represent a feasible and scalable therapeutic strategy for patients with early-stage AD. Collectively, our results may contribute to optimizing LDRT protocol for AD and also inspire the development of novel radiation systems employing low-dose X-ray beams within optimized energy, dose ranges, and dose rates for the treatment of AD and other neurodegenerative disorders.

Author Contributions: SL, YY, GK, SY, EK and JK: Methodology, Investigation, Formal Analysis. GK, EK and SY: Data Curation. SL: Writing—original draft. HR and WC: Methodology, Conceptualization, Supervision, Funding acquisition. All co-authors: Manuscript review, editing and approval.

Funding: This research was supported by the Basic Science Research Program through the National Research Foundation of Korea (NRF) funded by the Ministry of Science and ICT (No.: RS-2023-00253427 to W.C., 2022R1A2C3013138 to H.R.), by the Deep-Tech TIPS Program (No.: RS-2024-00467661) and the Startup Growth Technology Development Program (Didimdol Project) (No.: RS-2024-00441564) funded by the Ministry of SMEs and Startups (MSS, Korea), and by the H-Train Program through the Korea Innovation Foundation funded by the Ministry of Science and ICT (No.: RS-2025-02317308).

Institutional Review Board Statement: The study was conducted complying with the National Research Council's Guide for the Care and Use of Laboratory Animals and was approved by the Ethics Committee of Kyung Hee University Hospital at Gangdong (project identification code: KHNMC AP 2024-06, date: 30 July 2024).

Informed Consent Statement: Not applicable.

Data availability statement: The datasets generated and/or analyzed during the current study are available in the Supplementary Materials.

Acknowledgments: All co-authors would like to express our deepest gratitude to Dr. Jinho Choi, a medical physicist, for his faithful advice and review on this study. He provided expert advice, particularly on low-dose X-ray protocols.

Conflicts of Interest: All the authors declare that none of them have any conflicts on interest in relation to the current study.

Abbreviations

The following abbreviations are used in this manuscript:

AD	Alzheimer's disease
KLDR	kilovoltage low-dose radiation
MLDR	megavoltage low-dose radiation
LDR	low-dose radiation
LDRT	low-dose radiation therapy
PCR	polymerase chain reaction
ELISA	enzyme-linked immunosorbent assay
GFAP	glial fibrillary acidic protein
IL	interleukin
TNF	tumor necrosis factor
LPS	lipopolysaccharide

References

1. Vaiserman, A.; Cuttler, J. M.; Socol, Y., Low-dose ionizing radiation as a hormetin: experimental observations and therapeutic perspective for age-related disorders. *Biogerontology* **2021,** 22, (2), 145-164.
2. Baldwin, J.; Grantham, V., Radiation Hormesis: Historical and Current Perspectives. *Journal of nuclear medicine technology* **2015,** 43, (4), 242-6.

 doi:10.20944/preprints202604.0063.v1

3. Bevelacqua, J. J.; Mortazavi, S. M. J., Alzheimer 's Disease: Possible Mechanisms Behind Neurohormesis Induced by Exposure to Low Doses of Ionizing Radiation. *Journal of biomedical physics & engineering* **2018,** 8, (2), 153-156.
4. Paithankar, J. G.; Gupta, S. C.; Sharma, A., Therapeutic potential of low dose ionizing radiation against cancer, dementia, and diabetes: evidences from epidemiological, clinical, and preclinical studies. *Molecular biology reports* **2023,** 50, (3), 2823-2834.
5. Yin, E.; Nelson, D. O.; Coleman, M. A.; Peterson, L. E.; Wyrobek, A. J., Gene expression changes in mouse brain after exposure to low-dose ionizing radiation. *International journal of radiation biology* **2003,** 79, (10), 759-75.
6. Lowe, X. R.; Bhattacharya, S.; Marchetti, F.; Wyrobek, A. J., Early brain response to low-dose radiation exposure involves molecular networks and pathways associated with cognitive functions, advanced aging and Alzheimer's disease. *Radiation research* **2009,** 171, (1), 53-65.
7. Hautmann, M. G.; Rechner, P.; Neumaier, U.; Süß, C.; Dietl, B.; Putz, F. J.; Behr, M.; Kölbl, O.; Steger, F., Radiotherapy for osteoarthritis-an analysis of 295 joints treated with a linear accelerator. *Strahlentherapie und Onkologie : Organ der Deutschen Rontgengesellschaft ... [et al]* **2020,** 196, (8), 715-724.
8. Kim, S.; Chung, H.; Ngoc Mai, H.; Nam, Y.; Shin, S. J.; Park, Y. H.; Chung, M. J.; Lee, J. K.; Rhee, H. Y.; Jahng, G. H.; Kim, Y.; Lim, Y. J.; Kong, M.; Moon, M.; Chung, W. K., Low-Dose Ionizing Radiation Modulates Microglia Phenotypes in the Models of Alzheimer's Disease. *International journal of molecular sciences* **2020,** 21, (12).
9. Boyd, A.; Byrne, S.; Middleton, R. J.; Banati, R. B.; Liu, G. J., Control of Neuroinflammation through Radiation-Induced Microglial Changes. *Cells* **2021,** 10, (9).
10. Gao, C.; Jiang, J.; Tan, Y.; Chen, S., Microglia in neurodegenerative diseases: mechanism and potential therapeutic targets. *Signal transduction and targeted therapy* **2023,** 8, (1), 359.
11. Kim, S.; Nam, Y.; Kim, C.; Lee, H.; Hong, S.; Kim, H. S.; Shin, S. J.; Park, Y. H.; Mai, H. N.; Oh, S. M.; Kim, K. S.; Yoo, D. H.; Chung, W. K.; Chung, H.; Moon, M., Neuroprotective and Anti-Inflammatory Effects of Low-Moderate Dose Ionizing Radiation in Models of Alzheimer's Disease. *International journal of molecular sciences* **2020,** 21, (10).
12. Cuttler, J. M.; Moore, E. R.; Hosfeld, V. D.; Nadolski, D. L., Treatment of Alzheimer Disease With CT Scans: A Case Report. *Dose-response : a publication of International Hormesis Society* **2016,** 14, (2), 1559325816640073.
13. Cuttler, J. M.; Abdellah, E.; Goldberg, Y.; Al-Shamaa, S.; Symons, S. P.; Black, S. E.; Freedman, M., Low Doses of Ionizing Radiation as a Treatment for Alzheimer's Disease: A Pilot Study. *Journal of Alzheimer's disease : JAD* **2021,** 80, (3), 1119-1128.
14. Rogers, C. L.; Lageman, S. K.; Fontanesi, J.; Wilson, G. D.; Boling, P. A.; Bansal, S.; Karis, J. P.; Sabbagh, M.; Mehta, M. P.; Harris, T. J., Low-Dose Whole Brain Radiation Therapy for Alzheimer's Dementia: Results From a Pilot Trial in Humans. *International journal of radiation oncology, biology, physics* **2023,** 117, (1), 87-95.
15. Ceyzériat, K.; Zilli, T.; Fall, A. B.; Millet, P.; Koutsouvelis, N.; Dipasquale, G.; Frisoni, G. B.; Tournier, B. B.; Garibotto, V., Treatment by low-dose brain radiation therapy improves memory performances without changes of the amyloid load in the TgF344-AD rat model. *Neurobiology of aging* **2021,** 103, 117-127.
16. Ceyzériat, K.; Tournier, B. B.; Millet, P.; Dipasquale, G.; Koutsouvelis, N.; Frisoni, G. B.; Garibotto, V.; Zilli, T., Low-Dose Radiation Therapy Reduces Amyloid Load in Young 3xTg-AD Mice. *Journal of Alzheimer's disease : JAD* **2022,** 86, (2), 641-653.
17. Linnerbauer, M.; Wheeler, M. A.; Quintana, F. J., Astrocyte Crosstalk in CNS Inflammation. *Neuron* **2020,** 108, (4), 608-622.
18. Leng, F.; Edison, P., Neuroinflammation and microglial activation in Alzheimer disease: where do we go from here? *Nature reviews. Neurology* **2021,** 17, (3), 157-172.
19. Hur, J. Y.; Frost, G. R.; Wu, X.; Crump, C.; Pan, S. J.; Wong, E.; Barros, M.; Li, T.; Nie, P.; Zhai, Y.; Wang, J. C.; Tcw, J.; Guo, L.; McKenzie, A.; Ming, C.; Zhou, X.; Wang, M.; Sagi, Y.; Renton, A. E.; Esposito, B. T.; Kim, Y.; Sadleir, K. R.; Trinh, I.; Rissman, R. A.; Vassar, R.; Zhang, B.; Johnson, D. S.; Masliah, E.; Greengard, P.; Goate, A.; Li, Y. M., The innate immunity protein IFITM3 modulates γ-secretase in Alzheimer's disease. *Nature* **2020,** 586, (7831), 735-740.

 doi:10.20944/preprints202604.0063.v1

20. Hur, J. Y., Innate Immunity Protein IFITM3 in Alzheimer's Disease. *DNA and cell biology* **2021,** 40, (11), 1351-1355.
21. Friedlová, N.; Zavadil Kokáš, F.; Hupp, T. R.; Vojtěšek, B.; Nekulová, M., IFITM protein regulation and functions: Far beyond the fight against viruses. *Frontiers in immunology* **2022,** 13, 1042368.
22. Son, Y.; Lee, C. G.; Kim, J. S.; Lee, H. J., Low-dose-rate ionizing radiation affects innate immunity protein IFITM3 in a mouse model of Alzheimer's disease. *International journal of radiation biology* **2023,** 99, (11), 1649-1659.
23. Ismail, R.; Parbo, P.; Madsen, L. S.; Hansen, A. K.; Hansen, K. V.; Schaldemose, J. L.; Kjeldsen, P. L.; Stokholm, M. G.; Gottrup, H.; Eskildsen, S. F.; Brooks, D. J., The relationships between neuroinflammation, beta-amyloid and tau deposition in Alzheimer's disease: a longitudinal PET study. *J Neuroinflammation* **2020,** 17, (1), 151.
24. Wu, H. Y.; Kuo, P. C.; Wang, Y. T.; Lin, H. T.; Roe, A. D.; Wang, B. Y.; Han, C. L.; Hyman, B. T.; Chen, Y. J.; Tai, H. C., β-Amyloid Induces Pathology-Related Patterns of Tau Hyperphosphorylation at Synaptic Terminals. *Journal of neuropathology and experimental neurology* **2018,** 77, (9), 814-826.
25. Duyckaerts, C.; Delatour, B.; Potier, M. C., Classification and basic pathology of Alzheimer disease. *Acta neuropathologica* **2009,** 118, (1), 5-36.
26. Kent, S. A.; Spires-Jones, T. L.; Durrant, C. S., The physiological roles of tau and Aβ: implications for Alzheimer's disease pathology and therapeutics. *Acta neuropathologica* **2020,** 140, (4), 417-447.
27. Hampel, H.; Hardy, J.; Blennow, K.; Chen, C.; Perry, G.; Kim, S. H.; Villemagne, V. L.; Aisen, P.; Vendruscolo, M.; Iwatsubo, T.; Masters, C. L.; Cho, M.; Lannfelt, L.; Cummings, J. L.; Vergallo, A., The Amyloid-β Pathway in Alzheimer's Disease. *Molecular psychiatry* **2021,** 26, (10), 5481-5503.
28. LaFerla, F. M.; Green, K. N.; Oddo, S., Intracellular amyloid-beta in Alzheimer's disease. *Nature reviews. Neuroscience* **2007,** 8, (7), 499-509.
29. Ji, L.; Zhao, X.; Lu, W.; Zhang, Q.; Hua, Z., Intracellular Aβ and its Pathological Role in Alzheimer's Disease: Lessons from Cellular to Animal Models. *Current Alzheimer research* **2016,** 13, (6), 621-30.
30. Belley, M. D.; Ashcraft, K. A.; Lee, C. T.; Cornwall-Brady, M. R.; Chen, J. J.; Gunasingha, R.; Burkhart, M.; Dewhirst, M.; Yoshizumi, T. T.; Down, J. D., Microdosimetric and Biological Effects of Photon Irradiation at Different Energies in Bone Marrow. *Radiation research* **2015,** 184, (4), 378-91.
31. Bell, B. I.; Vercellino, J.; Brodin, N. P.; Velten, C.; Nanduri, L. S. Y.; Nagesh, P. K. B.; Tanaka, K. E.; Fang, Y.; Wang, Y.; Macedo, R.; English, J.; Schumacher, M. M.; Duddempudi, P. K.; Asp, P.; Koba, W.; Shajahan, S.; Liu, L.; Tomé, W. A.; Yang, W. L.; Kolesnick, R.; Guha, C., Orthovoltage X-Rays Exhibit Increased Efficacy Compared with γ-Rays in Preclinical Irradiation. *Cancer research* **2022,** 82, (15), 2678-2691.
32. Amols, H. I.; Lagueux, B.; Cagna, D., Radiobiological effectiveness (RBE) of megavoltage X-ray and electron beams in radiotherapy. *Radiation research* **1986,** 105, (1), 58-67.
33. Pattanayak, A.; Firdous, S. M., The 3xTg-AD Mouse Model: A Comprehensive Tool for Understanding Alzheimer's Disease. *Cellular and molecular neurobiology* **2026,** 46, (1), 41.
34. Drummond, E.; Wisniewski, T., Alzheimer's disease: experimental models and reality. *Acta neuropathologica* **2017,** 133, (2), 155-175.
35. Javonillo, D. I.; Tran, K. M.; Phan, J.; Hingco, E.; Kramár, E. A.; da Cunha, C.; Forner, S.; Kawauchi, S.; Milinkeviciute, G.; Gomez-Arboledas, A.; Neumann, J.; Banh, C. E.; Huynh, M.; Matheos, D. P.; Rezaie, N.; Alcantara, J. A.; Mortazavi, A.; Wood, M. A.; Tenner, A. J.; MacGregor, G. R.; Green, K. N.; LaFerla, F. M., Systematic Phenotyping and Characterization of the 3xTg-AD Mouse Model of Alzheimer's Disease. *Front Neurosci* **2021,** 15, 785276.
36. Kamatham, P. T.; Shukla, R.; Khatri, D. K.; Vora, L. K., Pathogenesis, diagnostics, and therapeutics for Alzheimer's disease: Breaking the memory barrier. *Ageing research reviews* **2024,** 101, 102481.
37. DeTure, M. A.; Dickson, D. W., The neuropathological diagnosis of Alzheimer's disease. *Molecular neurodegeneration* **2019,** 14, (1), 32.
38. Ceyzériat, K.; Zilli, T.; Millet, P.; Koutsouvelis, N.; Dipasquale, G.; Fossey, C.; Cailly, T.; Fabis, F.; Frisoni, G. B.; Garibotto, V.; Tournier, B. B., Low-dose brain irradiation normalizes TSPO and CLUSTERIN levels and promotes the non-amyloidogenic pathway in pre-symptomatic TgF344-AD rats. *Journal of neuroinflammation* **2022,** 19, (1), 311.

 doi:10.20944/preprints202604.0063.v1

39. Khan, A.; Sati, J.; Kamal, R.; Dhawan, D. K.; Chadha, V. D., Amelioration of cognitive and biochemical impairment in Aβ-based rodent model of Alzheimer's disease following fractionated X-irradiation. *Radiation and environmental biophysics* **2022,** 61, (2), 205-219.
40. Marples, B.; McGee, M.; Callan, S.; Bowen, S. E.; Thibodeau, B. J.; Michael, D. B.; Wilson, G. D.; Maddens, M. E.; Fontanesi, J.; Martinez, A. A., Cranial irradiation significantly reduces beta amyloid plaques in the brain and improves cognition in a murine model of Alzheimer's Disease (AD). *Radiotherapy and oncology : journal of the European Society for Therapeutic Radiology and Oncology* **2016,** 118, (1), 43-51.
41. Wilson, G. D.; Rogers, C. L.; Mehta, M. P.; Marples, B.; Michael, D. B.; Welsh, J. S.; Martinez, A. A.; Fontanesi, J., The Rationale for Radiation Therapy in Alzheimer's Disease. *Radiation research* **2023,** 199, (5), 506-516.
42. Yang, E. J.; Kim, H.; Choi, Y.; Kim, H. J.; Kim, J. H.; Yoon, J.; Seo, Y. S.; Kim, H. S., Modulation of Neuroinflammation by Low-Dose Radiation Therapy in an Animal Model of Alzheimer's Disease. *International journal of radiation oncology, biology, physics* **2021,** 111, (3), 658-670.
43. Wilson, G. D.; Wilson, T. G.; Hanna, A.; Fontanesi, G.; Kulchycki, J.; Buelow, K.; Pruetz, B. L.; Michael, D. B.; Chinnaiyan, P.; Maddens, M. E.; Martinez, A. A.; Fontanesi, J., Low Dose Brain Irradiation Reduces Amyloid-β and Tau in 3xTg-AD Mice. *Journal of Alzheimer's disease : JAD* **2020,** 75, (1), 15-21.
44. Kim, A.; Lee, J.; Moon, H.; Kim, C.; Yoo, M. Y.; Park, W. Y.; Kim, W. D.; Seo, Y. S., The effects of low-dose radiation therapy in patients with mild-to-moderate Alzheimer's dementia: an interim analysis of a pilot study. *Radiation oncology journal* **2023,** 41, (2), 89-97.
45. Koneru, B. N.; Sick, J.; Shaikh, H. A.; Spengler, H.; Small, W., Jr.; Shaffer, R., Low-Dose Radiation Therapy for Osteoarthritis: A Retrospective Single-Institution Analysis of 69 Patients and 168 Joints. *International journal of radiation oncology, biology, physics* **2025,** 123, (2), 352-360.
46. Faiz M. Khan, J. P. G., The Physics of Radiation Therapy, 5th ed. (2014). **2014**, 546-547.
47. Lillie, E. M.; Urban, J. E.; Lynch, S. K.; Weaver, A. A.; Stitzel, J. D., Evaluation of Skull Cortical Thickness Changes With Age and Sex From Computed Tomography Scans. *Journal of bone and mineral research : the official journal of the American Society for Bone and Mineral Research* **2016,** 31, (2), 299-307.
48. Kurkinen, M., Lecanemab (Leqembi) is not the right drug for patients with Alzheimer's disease. *Advances in clinical and experimental medicine : official organ Wroclaw Medical University* **2023,** 32, (9), 943-947.
49. Hall, E. J., Radiation dose-rate: a factor of importance in radiobiology and radiotherapy. *The British journal of radiology* **1972,** 45, (530), 81-97.